J. exp. Biol. 158, 117–132 (1991)
Printed in Great Britain © *The Company of Biologists Limited 1991*

SAILING DOWNWIND: AERODYNAMIC PERFORMANCE OF THE *VELELLA* SAIL

BY LISBETH FRANCIS

Biology Department, Bates College, Lewiston, ME 04240, USA

Accepted 7 March 1991

Summary

Using a wind tunnel built over a shallow pool and methods devised for measuring the performance of yacht sails, I describe aerodynamic performance *in situ* for the sailor-by-the-wind, *Velella velella*. By contrast with designers of the modern yacht mainsail, natural selection has apparently favored stability and seaworthiness over performance to windward. The *Velella* sail is a low aspect ratio airfoil with an unusually flat polar plot. Primarily a drag-based locomotory structure, this thin, leaf-like sail generates maximum force when oriented at attack angles between 50° and 90°. In the wind tunnel, free-sailing animals spontaneously assumed stable orientations at attack angles ranging from 28° to 87° and sailed with their hulls approximately broadside to the apparent flow of oncoming water. At these angles, aerodynamic force on the sail is asymmetrical, with the center of pressure upwind of the sail midline. Since aerodynamic force on the sail is balanced at equilibrium by hydrodynamic force on the hull, this orientation must be caused by asymmetrical forces acting on surface and underwater parts as the wind drags the animal along the surface of the water.

Introduction

Open ocean sailing is not exclusively a human pursuit. Among the pleuston, a suite of animals living at the air/water interface of the sea, two conspicuous cnidarians use wind power and an aerial sail to move along the surface. The deflatable aerial portion of the tropical man-of-war *Physalia physali* (L.) looks rather like a blue balloon topped by a long, puckered cock's comb (Totton and Mackie, 1960), while the fixed, thin, leaf-like sail of the sailor-by-the-wind *Velella velella* (L.) looks more like a conventional yacht sail (Fig. 1). The flat skeletal support of the *Velella* sail is permanently fixed to the chambered, gas-filled float; the flesh enveloping this skeleton has various muscular extensions, including a crest that can be either extended to increase the sail area or retracted to reef the sail.

Velella velella is a common member of the surface fauna from subarctic to subtropical waters. Huge numbers of these animals are often sighted at sea; in

Key words: airfoil, aspect ratio, Chondrophora, drag, locomotion, pleuston, wind, *Velella velella*.

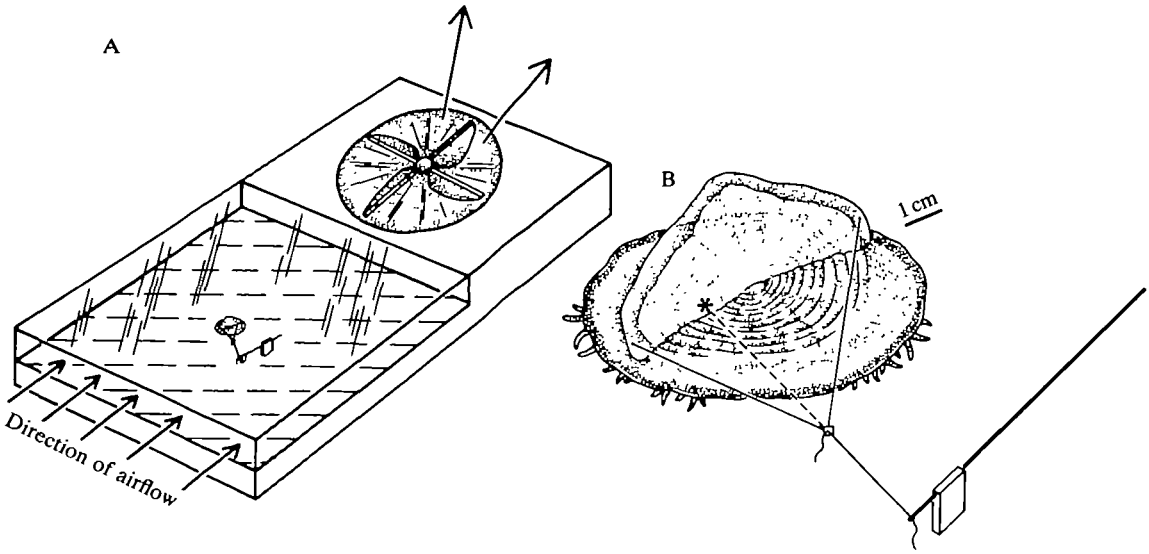

Fig. 1. The wind tunnel with a specimen of *Velella velella* tethered to the submerged force transducer. (A) A large fan creates steady and even airflow across a shallow pool of sea water 1.14 m along each side. (B) The tether line is attached to the free end of the wire, which is held in an underwater clamp and supported at the water's surface by a buoyant flag of plastic foam. The animal's orientation (measured as sail attack angle) can be changed by adjusting the length of one harness line where the free end dangles from the square friction fitting. Changing the attack angle causes lateral displacement of the center of pressure, measured as the distance from the sail midline to a point (asterisk) on the sail that is colinear (dotted line) with the tether line.

some localities, seasonal mass strandings litter the beaches with millions of their distinctive transparent skeletons. An asexual hydrozoan polyp (Mackie, 1959, 1962; Fields and Mackie, 1971), the sailor-by-the-wind lives attached to the air/water interface. In addition to harboring symbiotic algae, it feeds by dragging very short tentacles that comb the layer of water just below the surface, capturing fish and euphausid eggs, larvaceans and small crustaceans (Bieri, 1961). Each polyp buds off enormous numbers of tiny medusae that detach and reproduce sexually. Fertilized eggs develop through a (presumably) sinking larval phase to become buoyant, sailing polyps.

Older studies (Agassiz, 1833; Leloup, 1929) provide excellent descriptions of the gross anatomy and some information on development. More recently, Mackie (1959) and Fields and Mackie (1971) have investigated the neurophysiology and reinterpreted the anatomy on the basis of evolutionary considerations. Francis (1985) investigated the mechanical properties of the skeleton and structural support of the sail.

Like *Physalia* (but unlike most cnidarians) *Velella* shows marked right–left asymmetry associated with a tendency to sail at an angle to the downwind direction. The sail is set at about 40° to the long axis of the fleshy, elliptical ski

and along the short axis of the rhomboidal float (see photograph in Francis, 1985). Mackie (1962) found that specimens may sail at angles as much as 63° off the downwind direction.

Isomorphic forms exist with opposite (mirror-image) asymmetries. One form sails right of the downwind direction, while the other sails left of the wind (Woodcock, 1944; Bieri, 1959; Savilov, 1961; Mackie, 1962; Edwards, 1966). Bieri (1959), Savilov (1961) and Edwards (1966) studied the distribution of *V. velella* with special reference to the occurrence of the two oppositely sailing isomorphs.

There has been no detailed study of functional design as it relates to the orientation and movement of these animals. Because field work is so difficult and the anatomy of underwater soft parts so complex, the relative simplicity of sail design and function is particularly attractive as a point of attack. Here I describe aerodynamic performance of a *Velella* sail *in situ* using methods originally devised for measuring and comparing the performance of yacht sails (outlined in Marchaj, 1964).

Materials and methods

Collection and holding of specimens

Along the coast near Santa Cruz, California, northwesterly winds bring fresh specimens of *Velella velella* ashore fairly predictably each afternoon during the late spring and early summer months. During May and June of 1985–1988, healthy looking individuals were selected from among freshly stranded specimens reaching the beach at Davenport Landing (37°01′N, 122°15′W), placed in small containers with a little water and taken to the laboratory in an ice cooler.

In the laboratory, they were gently inverted under water to remove any trapped air bubbles from beneath the float and then floated upright on the surface of a large, shallow, fiberglass tank. Flowing sea water introduced at one end produced a slow eddy in the tank. The other end was screened off to keep animals away from the outflow area.

Testing was done as soon as possible, usually within 6 h after the animals had been collected. Although they readily ate small crustaceans and could sometimes be kept for up to a week, the animals tended to deteriorate rather quickly in the laboratory. Within a few days, tissue covering the sail usually became dehydrated; and the fleshy floating skirt began to disintegrate. Animals collected at sea fared no better than those collected from the beach.

Definition of terms

An airfoil is a body with flat or curved surfaces that generate lift as it moves through the air. One descriptor of airfoil shape is the aspect ratio (AR), the ratio of length to width. A convenient formula for the aspect ratio of odd-shaped sails is the square of maximum sail height (H^2) divided by planform sail area (S): ($AR=H^2/S$). Orientation of an airfoil is described by the attack angle, the angle of inclination relative to mass flow. Defined for my purposes here, sailing angle is the

direction of motion relative to mass airflow. For example, if unanchored, an empty canoe typically orients broadside to the wind (attack angle=90°) and blows straight downwind (sailing angle=0°).

The vector sum of local aerodynamic forces acting on an airfoil is the resultant force; and its point of application is the center of pressure. Resultant force is often separated into two or more orthogonal components, lift and drag. Where lift or crosswind force is a component acting perpendicular to mass airflow, drag or downwind force is a component acting parallel to the wind. Commonly described sources of aerodynamic drag include parasite drag on body parts other than the airfoil, form drag and friction drag on the airfoil itself, and induced drag, a component of form drag associated with lift generation and the formation of tip vortices.

Force coefficients (C_F) are dimensionless numbers used in describing and comparing the effects of airfoil shape on aerodynamic performance: $C_F=2F/\rho SU^2$, where F is force, ρ is fluid density, U is mainstream fluid velocity and S is some characteristic area of the airfoil (planform area, in this case).

The wind tunnel

Animals were tested in a wind tunnel where a variable-speed fan created an even flow of air across the surface of a level pool 114 cm long, 114 cm wide and 10 cm deep (Fig. 1). Observations were made through a sheet of plate glass that roofed the tunnel 16 cm above the water's surface, and a plastic grid on the bottom of the tank served for reference.

Ambient sea water flowed into the tank slowly through an inlet at the upwind end and overflowed at the downwind end *via* a standpipe that also skimmed off surface debris. Since my specimens all sailed left of the wind, the plumbing was placed to the far right of the tank so that testing could be done well away from these areas of higher water flow.

A turbine-style anemometer was routinely used to measure mainstream wind velocities at the upwind end of the tank, and a hot-wire anemometer was also used initially to check for evenness of flow across the width. By sailing floating balls and a variety of plastic models, I confirmed that the airflow remained unidirectional throughout the tank.

The force transducer

Aerodynamic force on the sail was measured in the wind tunnel by tethering an animal to the free end of a springy piece of steel wire which served as a force transducer. A piece of piano wire of suitable thickness was chosen and its length adjusted so that maximum deflections during testing were less than 10% of the exposed wire length (i.e. conveniently within the linear portion of the force/deflection curve). The fixed end of the barely submerged wire was held parallel to the water's surface in an underwater clamp. Being under water isolated the transducer from the direct effects of the wind and prevented any interference with windflow patterns. The free end of the wire was supported by a small buoyant flag

compressed plastic foam, which prevented it from drooping and tended to damp oscillations (Fig. 1). Force on the sail caused deflection of the wire tip that could be measured with a ruler.

The transducer was calibrated in air by lowering the fixed end in measured increments while the free end of the wire rested on the pan of an electronic balance. Weight changes associated with a series of tip deflections were used to construct a force/deflection curve.

With this simple mechanical device it was possible to measure surprisingly small forces. A force of 4.67×10^{-5} N (4.76 mg) caused a 1 mm deflection in the tip of the wire, which was 244 mm long and 0.45 mm thick.

Morphometrics

As an indication of individual size, the maximum width (W) of the sail was routinely measured for all animals by using a pair of calipers to span the widest part of the sail. For the animal used in static testing, and for nine individuals collected haphazardly in June 1988, maximum height (H) and planform area (S) were also measured from an outline of the amputated sail skeleton. These measurements were used to calculate aspect ratios (H^2/S).

Although the animals commonly erected their crests in the holding tank, where there was continual water flow and little air movement, the muscular sail crest was not erected during tests in the wind tunnel. For this reason, sail dimensions reported here are for the reefed sail with the crest not erected.

Wind velocity and Reynolds number

During testing, the wind velocity measured 6 cm above the water was $1.3\,m\,s^{-1}$ (about 2.5 knots) and the Reynolds number based on maximum sail width was about 4000. While large ripples or vigorous wind-driven circulation of water in the tank could potentially cause errors in the force measurements, surface ripples were actually quite small; circulation in the tank was undetectable using dye streams. Since the sail remained fully upright (no obvious tilting of the animal or bending of the sail during testing), aerodynamic force on the sail was assumed to be horizontal.

Static testing

Magnitude and direction of the resultant force

A moderately large specimen was connected to the force transducer using one pound test, monofilament fishing line sewn through the ends of the sail and fastened with simple friction fittings (tiny pieces of rubber band) to form an adjustable harness and tether (Fig. 1). Attack angle was adjusted by shortening or lengthening one of the harness lines. With the transducer wire oriented perpendicular to the tether line (and thus to the resultant force), I recorded tip deflections at a series of attack angles, then amputated the sail and repeated the series of measurements. Tip deflections were later converted to force in newtons.

Attack angle, center of pressure and direction of the resultant force

With the animal tethered in the wind tunnel, I adjusted the harness lines to obtain various attack angles, took photographs from directly above, and from these measured the attack angle of the sail, the angle of the tether line (which is colinear with the resultant force vector) and lateral displacement of the center of pressure (distance between the sail midline and a point on the sail colinear with the tether line, expressed as a fraction of the maximum sail width).

Dynamic testing

Average sailing direction, sailing velocity and attack angle were measured on freely moving individuals. Eight moderately large animals were collected haphazardly between 14 June and 3 July 1987, returned to the laboratory and tested in the wind tunnel.

To avoid disturbing the tentacles, each animal was gently transferred to the upwind end of the wind tunnel in a small fingerbowl. A flat paddle inserted and withdrawn through a slot in the top of the wind tunnel made it easy to position and release each animal uniformly, with the sail broadside to the wind. Once its orientation became stable and the animal stopped accelerating, the average direction of motion, attack angle, straight-line distance traveled and the time to travel that distance were measured directly using a stopwatch, a protractor and a meter stick.

Results

Morphometrics

The sail of the animal used in static tests was 57 mm wide at the base and 24 mm high in the middle, with a planform area of 835 mm^2 and aspect ratio (H^2/S) of 0.69. For convenience and consistency, specimens used in testing were all moderately large individuals. Maximum sail widths for the eight specimens used in the dynamic tests ranged from 50 to 63 mm. The mean aspect ratio$\pm$1 S.D. for nine haphazardly collected specimens (maximum sail lengths between 32 and 77 mm) was 0.56$\pm$0.1. There was no obvious relationship between size and aspect ratio within this size range.

Static test results

Attack angle and horizontal force

Figs 2, 3 and 4 show the effects of sail orientation (attack angle) on all three vector properties: (1) the magnitude of the horizontal resultant force (Fig. 2), (2) the direction of the aerodynamic force (Fig. 3) and (3) the lateral position of the center of pressure (Fig. 4).

Total aerodynamic force is greatest at attack angles above 50°, and declines fairly steeply as the attack angle is decreased below about 50° (Fig. 2). While drag decreases with the attack angle, lift increases; and so lift contributes more strongly

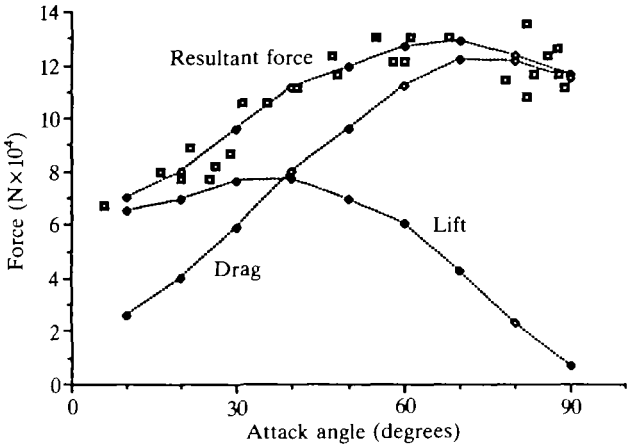

Fig. 2. Total (horizontal) aerodynamic force acting on a moderately large specimen of *Velella velella* (maximum sail length, 57 mm) at near-surface windspeeds of $1.3\,m\,s^{-1}$, measured as a function of the animal's orientation (attack angle of the sail). A line was fitted by connecting average points (small squares) calculated after rounding attack angles to the nearest 10°. Lift and drag components were calculated from direct measurements of force magnitude and direction.

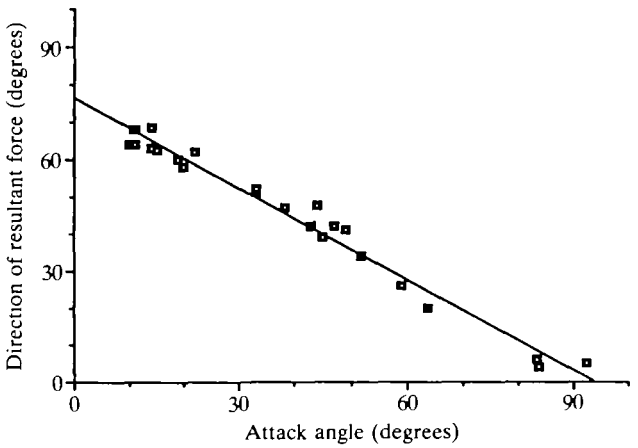

Fig. 3. Direction of the aerodynamic force acting on a moderately large specimen of *Velella velella* as a function of the attack angle of the sail; ($y=-0.8x+76.7$; $r=0.99$). Force direction is measured as a counterclockwise angle in relation to wind direction.

to total horizontal force at more acute angles of attack. The relationships here are clearly not linear, and curves were fitted by connecting average points calculated after rounding attack angles to the nearest 10°.

The relationship between attack angle and the direction of the resultant force is linear (Fig. 3; line fitted by least-squares regression: $y=-0.8x+76.7$; $r=0.99$).

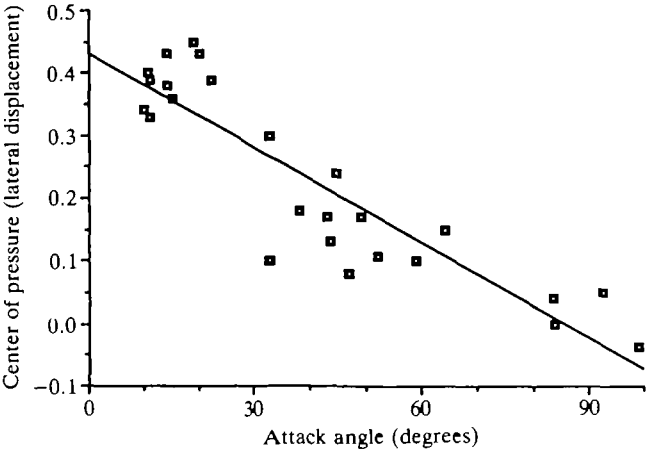

Fig. 4. Displacement of the aerodynamic center of pressure from the sail midline (with the sail broadside to the wind) towards the upwind end of the sail (with decreasing attack angle), expressed as a fraction of sail width, and measured as a function of sail attack angle ($y=-0.005x+0.43$; $r=0.90$).

With the sail broadside (attack angle, 90°), the animal is pushed straight downwind (direction of the resultant force, 0°). As the attack angle decreases, force on the sail is directed at increasingly greater angles to the left of the downwind direction.

The relationship between attack angle and the lateral displacement of the center of pressure is roughly linear within the range of attack angles examined (Fig. 4; $y=-0.005x+0.43$; $r=0.90$). With the sail broadside to the wind, the center of pressure is at the midline. As the attack angle is decreased, the center of pressure moves increasingly upwind, towards the leading edge of the sail.

Attack angle and force coefficients

Polar diagrams for the *Velella* sail and for model boat sails of various shapes (modified after Marchaj, 1964) are shown in Fig. 6. A line was fitted to the *Velella* data by connecting average points calculated after rounding attack angles to the nearest 10°.

Parasite drag

Aerodynamic force on the animal without its sail was 1.5×10^{-4} N, regardless of the orientation; the parasite drag coefficient (based, for convenience, on sail planform area) was estimated at 0.18.

Dynamic test results

Orientation, velocity and sailing direction

Under test conditions (near-surface windspeeds of $1.3\,m\,s^{-1}$), the average terminal velocity was $4.6\pm0.6\,cm\,s^{-1}$ (mean±standard deviation) for eight model

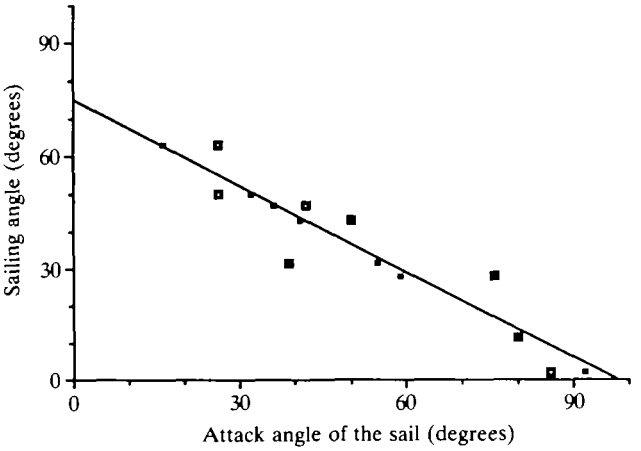

Fig. 5. Spontaneous orientation and sailing direction of eight freely sailing specimens of *Velella velella* measured in the wind tunnel. The line ($y=-0.76x+75.0$; $r=0.91$) was fitted to the data points (large squares) using least-squares regression. For comparison, attack angles producing a resultant force in the direction of motion (taken from static test results) are also given for each animal (small squares).

ately large, healthy animals sailing smoothly with the sail crests not erected. Spontaneous orientation resulted in attack angles ranging from 28° to 87°, with the corresponding sailing angles ranging from 64° to 3° left of the wind. Because the animals move so slowly, the apparent windspeed and direction are virtually identical with the actual windspeed and direction.

The relationship between average attack angle and sailing direction is shown in Fig. 5 (large squares). Sailing angle increased linearly with decreasing attack angle, and the attack angle and sailing angle are approximately complementary. Although dynamic test results were more variable than static test results, on average the animals moved in the direction of the resultant force, as measured during static testing (Fig. 3; Fig. 5, small squares).

Discussion

The lift-generating locomotory structure of *Velella velella* looks and performs more like a boat sail than a bird wing. With the animal's weight resting on the water's surface, the sail need only generate sufficient propulsive force to balance hydrodynamic drag. By contrast, a wing must also generate lift sufficient to balance the weight of the animal in order to keep it aloft (Leyton, 1975).

Yachts can sail upwind and are generally designed to maximize this capacity. By contrast, *V. velella* sails only downwind. This specialization is clearly reflected in the design of the tiny sail, which is bilaterally symmetrical and stubby rather than being asymmetrical, tall and narrow like the typical modern mainsail.

Sail performance and design

Long, slim airfoils with relatively high aspect ratios are generally advantageous where adequate performance requires relatively large lift forces accompanied by little drag. This is generally the case for large airfoils operating at relatively acute angles of attack (e.g. the wings of large, soaring birds and yacht mainsails).

For modern yacht mainsails, where the aspect ratio (H^2/S) commonly approaches 4, the polar diagram (Fig. 6) shows a sharp peak in the resultant force coefficient at low attack angles, followed by a sudden drop in the lift coefficient as the attack angle is increased beyond the angle of optimum performance and the separation point suddenly moves upwind. For sails with progressively lower aspect ratios (Fig. 6), the curve becomes more flattened, stalling is increasingly delayed, and maximum force occurs at higher attack angles.

In comparing shape and performance of the *Velella* sail and of yacht sails, I have chosen to use the common, geometric formula for the aspect ratio (H^2/S=0.7 for *V. velella*) as a simple descriptor of shape. Those wishing instead to compare the

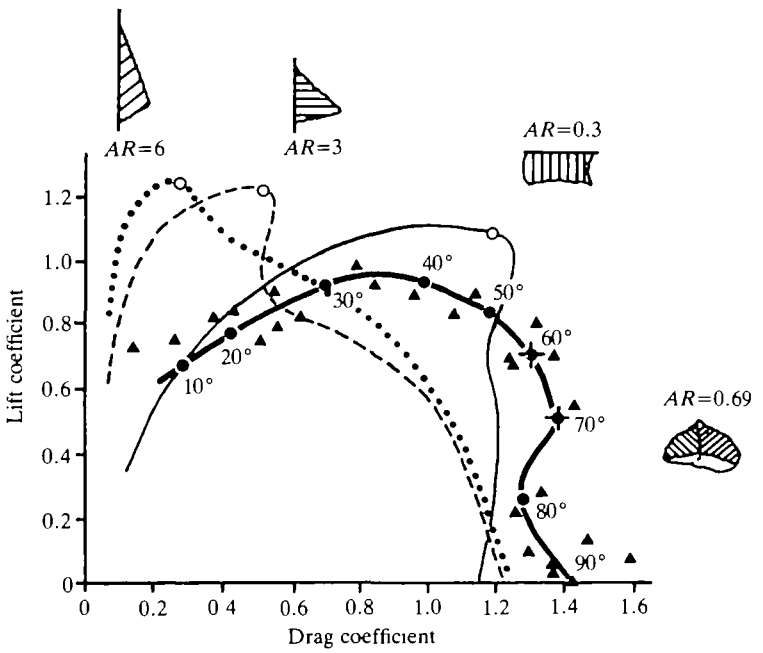

Fig. 6. Polar diagram for *Velella velella* (AR=0.69) showing lift and drag coefficients as a function of sail attack angle, given in 10° increments. Individual data points (▲) were computed from measurements of force magnitude and direction (Figs 2 and 3), and a line was fitted by connecting average points (●) calculated after rounding attack angles to the nearest 10°. The resultant coefficient (distance from the origin) is highest at attack angles between 60° and 70° (marked by a cross over the black dot). For comparison, polar plots for model sails of various shapes are redrawn from Marchaj (1964) (aspect ratios and sketches are next to the peak for each polar plot, marked by a white circle).

characteristics of bird, bat or insect wings may prefer to use the formula specifically modified to reflect effective performance of an attached airfoil (Marchaj, 1964) ($2H^2/S$=1.4 for *V. velella*).

By any standard, the *Velella* sail is a low aspect ratio airfoil; its polar plot shows the characterictic flattened shape (Fig. 6). The resultant coefficient is highest at very large attack angles, and there is no abrupt decrease in lift coefficient with increasing attack angle. However, the *Velella* sail produces more drag and less lift at moderate attack angles than might be expected for an airfoil of this shape, especially for an attached airfoil which has only one tip vortex and thus half the quota of induced drag of a yacht sail.

Source of the driving force

Drag, rather than lift, is usually the major aerodynamic component acting on the *Velella* sail. This is clear both from the movement of free-sailing individuals and from static measurements of force magnitude and direction. The Reynolds number calculated for this test situation (Re=4000) suggests that profile drag should be more important than friction drag by about three orders of magnitude (Vogel, 1981). As the attack angle of an airfoil is increased, the projected area (or profile) increases as the sine of the attack angle; thus, profile drag should increase with attack angle to a maximum at 90°, as it does in this case.

Some portion of the broad, lower part of the sail (as well as the upper surface of the hull and skirt) must operate in the boundary layers of increasingly reduced windspeed near the air/water interface. It is possible, therefore, that friction drag contributes more to the transfer of energy in this situation than is ordinarily the case at Reynolds numbers in the thousands. Where the local Reynolds number falls below about 100, friction drag will account for a significant proportion of the drag for that region. However, reduced windspeed generally means reduced aerodynamic force, and the bottom few millimeters of the sail probably do not contribute a large proportion of the total drag at these velocities.

Parasite drag (on the upper surfaces of the float and skirt) can also contribute to effective aerodynamic force. Although the skirt of *V. velella* conforms quite closely to the water's surface, the hull does project slightly. Drag on the body after the sail had been amputated was 10–18 % of the total aerodynamic drag measured on the intact animal. Because the presence of the sail affects the pattern of flow around the body, this may or may not be a good estimate of the actual parasite drag acting on an intact animal at this windspeed.

Except at attack angles of 0° or 90° (where resultant force can be straight downwind), lift also contributes to the resultant force. Lift on the *Velella* sail decreases if the attack angle is increased beyond about 40° (Fig. 2). However, lift coefficients are substantially lower for the *Velella* sail than for any of the model sails, including the rectangular sail with a very low aspect ratio (0.3). In addition to being rather short and squat, the *Velella* sail tapers abruptly to a point at the top. For yacht sails, a pointed tip accentuates the relative importance of the tip vortex

and induced drag (Marchaj, 1988), which, in turn, interfere with the generation of lift.

Induced drag increases with lift and is relatively important for low aspect ratio airfoils like the *Velella* sail, because airflow over much of the airfoil is grossly influenced by the tip vortex (Marchaj, 1988). Measurement of the induced drag for another low aspect ratio airfoil ($AR=1$), demonstrated that this component is significant (exceeding 5% of the total drag) when the lift coefficient is 0.4 or greater (Marchaj, 1988), which applies at attack angles of less than 75° for the *Velella* sail. Addition of this induced component at moderately high attack angles (60° −75°) may explain the broad, flat peak in total drag occurring at attack angles between 60° and 90° (Fig. 2) for this stubby airfoil.

While drag tends to reduce the effectiveness of lift-based locomotory structures (reducing the ground-speed of a gliding hawk, for example), induced drag, parasite drag and friction drag all contribute to the driving force for any drag-based locomotion. Inclusion of parasite drag in the measurement of total force may help to explain why both drag and total force coefficients are higher for *Velella* than for the model sails (Fig. 6).

Large coefficients and high speeds

Large force coefficients imply efficient capture of wind energy and potentially high sailing speeds. However, while yachtsmen are inveterate thrill seekers, there is no reason to assume that high speed is particularly advantageous for *Velella*.

At relatively low wind velocities, efficient use of windpower almost certainly improves feeding efficiency. Dragging tentacles through the water, rather than simply drifting along with it, should increase the rate of encounter with potential prey. At windspeeds below about $0.3\,m\,s^{-1}$ ($Re<100$), friction drag will significantly affect aerodynamic performance, presumably resulting in more efficient transfer of energy and, consequently, in higher drag and resultant coefficients than those measured here.

At higher wind velocities, the larger aerodynamic and hydrodynamic forces associated with faster sailing may actually become a problem. Above some optimum speed, hydrodynamic drag will probably produce undesirable distortions in the soft tentacles and blastostyles, making the animals less effective as food traps. Under heavy weather conditions, very high force on the sail could cause extreme tilting, leading to capsizing.

Seaworthiness and sail shape

Of the performance features usually discussed by yacht designers, seaworthiness seems particularly relevant. When overturned, the animals cannot right actively, although voluntary changes in posture increase the likelihood that chance interactions of waves and gusting wind will cause righting. Under laboratory conditions, individuals that remain upside down or on their sides for a few hours apparently undergo degenerative changes and are subsequently unable to maintain the normal, upright posture (L. Francis, personal observation).

Two obvious features of sail design should contribute to this animal's relative stability – the tapered shape of the sail and the low aspect ratio (Francis, 1985). For short squat sails, the center of pressure is relatively near the waterline. In addition, the tapering *Velella* sail, which is narrower at the tip and broader at the base, has a relatively lower center of pressure than a rectangular sail with the same aspect ratio. A low center of pressure means relatively high stability. Tipping is caused by heeling moment, which is horizontal force times the moment arm (distance from the center of pressure on the sail to the center of resistance for surface and under water parts). With its center of pressure near the waterline, *Velella* should be relatively stable.

Little is known about the behavior and sailing performance of *Velella velella* under open ocean conditions, or about the patterns of near-surface air flows with which it interacts. However, sailors and windsurfers consistently report that, in windspeeds up to about $10\,m\,s^{-1}$ (20 knots), the animals sail along relatively smoothly; in $15\,m\,s^{-1}$ winds (30 knots), they spin more or less continuously; in $20\,m\,s^{-1}$ winds (40 knots), they tumble end-over-end (Mackie, 1962; J. Risser and W. Jarmann, personal communication).

Windspeed in the laboratory and in the field

What field conditions might produce the near-surface windspeeds experienced by animals in the wind tunnel? We can only guess. Given the obvious difficulties involved in obtaining measurements within a few centimeters of the ocean's surface, and while admitting that actual complexity and variability prevent realistic prediction either from theory or by extrapolation, it does seem worthwhile to attempt at least a rough calculation.

The standard equation of the micrometeorologist describes a logarithmic increase in windspeed with increasing height: $U_x = U^*/k \cdot \ln[(z-d)/z_o]$, where U_x is wind velocity at height z, U^* is the friction velocity, k is Von Karman's constant, d is the zero ground displacement and z_o is the roughness parameter (Vogel, 1981). This equation has been found to apply reasonably well over open water, at least under some conditions (Sutton, 1953).

In the wind tunnel, the water's surface was relatively smooth, and a velocity of $1.3\,m\,s^{-1}$ was measured 6 cm above the water's surface. By substituting arbitrary, but ordinary, values for the friction velocity ($U^*=0.8$) and zero ground displacement ($d=0.04$m), the standard, empirically determined value for the Von Karman's constant ($k=0.4$) and a small value for the roughness parameter ($z_o=0.01$), the windspeed predicted at 6 cm is $1.3\,m\,s^{-1}$ (2.5 knots), at person height of 2 m, about $11\,m\,s^{-1}$ (21 knots) and at the yachtsman's standard height of 10 m, about $14\,m\,s^{-1}$ (27 knots). This would be a strong breeze (6 on the Beaufort scale), described by Marchaj (1964) on his psychological scale for sailors as inducing 'delight tinged with anxiety'. Standard charts predict waves up to 6 m high under these conditions.

The fact that the animals reefed their sails during testing also suggests that they

are moving at or beyond some optimal sailing velocity, or that ordinarily there may be significant risk of capsizing under these conditions.

Sail orientation and sail shape

In steady, unidirectional flow, a bilaterally symmetrical sheet that is free to rotate about a central pivot point (e.g. the *Velella* sail with a tether attached at the midline, or a sheet of plywood that is lifted by grasping both edges) will spontaneously orient broadside to flow, in the drag-maximizing position. This orientation is stable, because the center of pressure is at the midline and aerodynamic force is colinear with the resistance provided by the central pivot point. Displacement to any other orientation results in asymmetrical aerodynamic force on the sail, rotation (the center of pressure moves upwind and the resultant force is no longer colinear with the central pivot point) and return to the equilibrium position, broadside. Like weathervanes, yacht mainsails are generally asymmetrical, and (without the asymmetrical hydrodynamic resistance provided by a keel) would spontaneously assume the drag-minimizing position, with the sail oriented edge-on into the wind.

Although the *Velella* sail is bilaterally symmetrical, freely moving specimens rarely orient with the sail exactly broadside to the wind because the shape of the hull and skirt produces asymmetrical hydrodynamic forces on surface and underwater parts as the animal moves through the water.

Sail orientation and hydrodynamic resistance

The animals assume a stable orientation (no rotation) and move at a constant velocity (no acceleration) when the aerodynamic force acting on aerial parts is balanced by the hydrodynamic force acting on surface and underwater parts. Constant velocity is achieved when the magnitudes of the hydrodynamic and aerodynamic force resultants are equal. Stable orientation in the horizontal plane can be achieved when the hydrodynamic and aerodynamic centers of pressure are coincident or when the hydrodynamic and aerodynamic force vectors are colinear and opposed (ignoring vertical differences, which cause tilting). Unless the animals are sailing straight downwind, the hydrodynamic center of pressure (like the aerodynamic center of pressure) must be asymmetrical with respect to the animal's primitive axis of symmetry through the sail midline.

Thus, it is possible to conclude that freely moving specimens of *Velella velella* orient with their sails at various acute angles of attack because of asymmetrical and individually variable hydrodynamic forces acting on their wetted under surfaces (L. Francis, in preparation).

Control of orientation and sailing direction

In addition to reefing or extending the sail edge, the animals might increase or reduce the efficiency of the sail as a locomotory structure by adjusting the attack angle. Since resultant force is highest at attack angles between 50° and 90° (Fig. 2), force on the *Velella* sail could be maximized under calm and light wind

conditions by orienting the sail nearly broadside to the wind. In strong winds, reducing the attack angle to less than 50° would reduce pressure on the sail, sailing speed, hydrodynamic forces and the likelihood of capsizing.

During dynamic tests, freely moving individuals assumed stable orientations at attack angles ranging from 26° to 87°. Work in progress suggests that the animals can change their orientation and sailing direction to some extent (suggested by Mackie, 1962) by changing the posture of underwater parts affecting the hydrodynamic force (L. Francis, in preparation).

It is perhaps worth noting that the aerodynamic attack angle and the sailing angle are always approximately complementary. This means that the hydrodynamic attack angle (the orientation of hull and tentacles relative to the apparent water flow=aerodynamic attack angle+sailing angle) is always approximately 90°. Consequently, the rows of short, curved feeding tentacles attached beneath the edge of the submerged hull tend to fish the same, broad swath, regardless of how the sail may be oriented relative to the wind.

I thank directors, staff and colleagues at Long Marine Laboratory, Friday Harbor Laboratories, Duke University Zoology Department and Shannon Point Marine Center for providing space, assistance, ideas and equipment during the study. In particular, I thank S. A. Wainwright, S. Vogel, B. Best, J. Voltzow, K. Skaug, C. Smith, and R. L. Self for help in designing and building various versions of the wind tunnel, and B. Clark, M. W. Denny, S. J. Feldcamp, G. O. Mackie, P. H. Risser and an anonymous reviewer for particularly useful discussion. Special thanks to the late Robert Bieri, teacher, colleague and fellow traveler.

References

AGASSIZ, A. (1833). Exploration of the surface fauna of the Gulf Stream III, Part I. The *Porpitidae* and *Velellidae*. *Mem. Mus. comp. Zool. Harvard* **8**, 1–16.

BIERI, R. (1959). Dimorphism and size distribution in *Velella* and *Physalia*. *Nature* **184**, 1333.

BIERI, R. (1961). Post-larval food of the pelagic coelenterate, *Velella lata*. *Pacific Sci.* **15**, 553–556.

EDWARDS, C. (1966). *Velella velella* (L.): The distribution of its dimorphic forms in the Atlantic Ocean and the Mediterranean, with comments on its nature and affinities. In *Some Contemporary Studies in Marine Science* (ed. H. Barnes), pp. 283–296. New York: Hafner.

FIELDS, W. G. AND MACKIE, G. O. (1971). Evolution of the Chondrophora: Evidence from behavioral studies on *Velella*. *J. Fish. Res. Bd Can.* **28**, 1595–1602.

FRANCIS, L. (1985). Design of a small cantilevered sheet: the sail of *Velella velella*. *Pacific Sci.* **39**, 1–15.

LELOUP, E. (1929). Recherches sur l'anatomie et le developpement de *Velella spirans* Forsk. *Archs Biol.* **39**, 397–478.

LEYTON, L. (1975). *Fluid Behavior in Biological Systems*. Oxford: Clarendon Press.

MACKIE, G. O. (1959). The evolution of the Chondrophora (Siphonophora–Disconanthae): new evidence from behavioral studies. *Trans. R. Soc. Can.* **53**, 7–20.

MACKIE, G. O. (1962). Factors affecting the distribution of *Velella* (Chondrophora). *Int. Rev. ges. Hydrobiol.* **161**, 26–32.

MARCHAJ, C. A. (1964). *Sailing Theory and Practice*. New York: Dodd, Mead and Co.

MARCHAJ, C. A. (1988). *Aero-Hydrodynamics of Sailing*. Camden, Maine: International Marine Publishing.

SAVILOV, A. I. (1961). The distribution of the ecological forms of the by-the-wind sailor, *Velella lata* Ch. and Eys. and the Portuguese Man-of-War, *Physalia utriculus* (La Martiniere) Esch., in the North Pacific. *Trudy Inst. Okeanol. Akad. Nauk SSSR* **45**, 223–239.

SUTTON, O. G. (1953). *Micrometeorology. A Study of Physical Processes in the Lowest Layers of the Earth's Atmosphere*. New York: McGraw-Hill Co., Inc.

TOTTON, A. K. AND MACKIE, G. O. (1960). Studies on *Physalia physalis* (L.). *Discovery Reports* **30**, 371–407.

VOGEL, S. (1981). *Life in Moving Fluids*. Boston: Willard Grant Press.

WOODCOCK, A. H. (1944). A theory of surface water motion deduced from the wind-induced motion of *Physalia*. *J. mar. Res.* **5**, 196–205.